

Large optical nonlinearity of Au nanoparticle-dispersed $\text{Ba}_{0.6}\text{Sr}_{0.4}\text{TiO}_3$ films prepared by pulsed laser deposition

Cong Chen², Tingyin Ning¹, Yueliang Zhou^{1,3}, Dongxiang Zhang¹,
Pei Wang², Hai Ming² and Guozhen Yang¹

¹ Laboratory of Optical Physics, Institute of Physics, Chinese Academy of Sciences, PO Box 603, Beijing, 100190 People's Republic of China

² Anhui Key Laboratory of Optoelectronic Science and Technology, University of Science and Technology of China, Hefei, Anhui, 230026 People's Republic of China

E-mail: ylzhou@aphy.iphy.ac.cn

Received 3 July 2008, in final form 18 September 2008

Published 23 October 2008

Online at stacks.iop.org/JPhysD/41/225301

Abstract

Crystallized Au nanoparticle-dispersed $\text{Ba}_{0.6}\text{Sr}_{0.4}\text{TiO}_3$ (Au : BST) thin films were prepared on MgO (1 0 0) substrates by pulsed laser deposition. The peak of the linear absorption coefficient for the film shifts to longer wavelength with an increase in Au concentration. Among all the tested samples, the largest values of third-order nonlinear susceptibility were calculated to be -1.93×10^{-6} esu and 1.13×10^{-5} esu corresponding to imaginary and real parts, respectively, which were determined by a single beam Z-scan at a wavelength of 532 nm with a laser duration of 10 ns. The relationship between Au concentration and third-order nonlinear susceptibility was also analysed.

(Some figures in this article are in colour only in the electronic version)

1. Introduction

Materials with large third-order optical nonlinear susceptibility have been of growing interest in recent years [1] because of their potential application in optical switches, optical computing, real time holography, optical correlators and phase conjugators [2]. It has been reported that barium titanate (BaTiO_3) doped with certain elements such as Ce, Au and Rh shows a large nonlinear optical response [3–5]. Meanwhile, the magnitude of the third-order nonlinear susceptibility of Cu nanoparticle-dispersed $\text{Ba}_{0.6}\text{Sr}_{0.4}\text{TiO}_3$ (Cu : BST) films on Al_2O_3 (0 0 1) substrates was calculated to be 9.737×10^{-9} esu [6]. In such nanocomposite systems, large optical nonlinearity arises primarily from a strong local field effect and anisotropic effect because of irregular metal nanoparticles [7–11].

There are several methods to produce metal nanocomposite films such as ion implantation [12], sol–gel [13], sputtering [14] and pulsed laser deposition (PLD) [15]. In this study, PLD was used to produce thin films. It is a flexible tool and has

shown great potential for the development of thin films with good adhesion and high density. What is more, PLD provides easy control of the stoichiometry and enables us to prepare thin films with different metal concentration.

This paper reports the fabrication and third-order optical nonlinearity of Au nanoparticle-dispersed $\text{Ba}_{0.6}\text{Sr}_{0.4}\text{TiO}_3$ (Au : BST) films on MgO (1 0 0) substrates deposited at 750 °C by the PLD technique. The third-order optical nonlinearity susceptibility was determined by the Z-scan method [16, 17] at a wavelength of 532 nm with a laser duration of 10 ns. It also shows the red-shift of linear absorption peak with increase in Au concentration. The relationship between nonlinear optical properties and Au concentration has been given.

2. Experimental details

Au : BST nanocomposite films were prepared on MgO (1 0 0) substrates using PLD with a Lambda Physik XeCl excimer laser (308 nm, 20 ns full width at half maximum). A fan-shaped chip of 99.999% metal Au was placed onto a sintered

³ Author to whom any correspondence should be addressed.

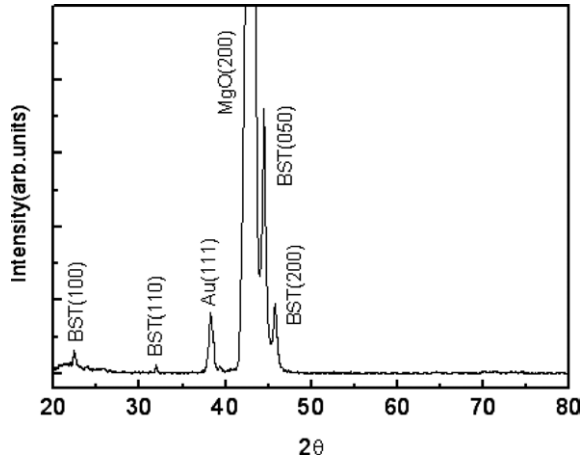


Figure 1. XRD θ - 2θ scan of the Au:BST films.

BST target mounted on a rotating holder, 4 cm from the substrates. The pulsed laser was focused on the target at a typical energy density of about 2 J cm^{-2} with a 4 Hz repetition rate. During the deposition process, Au and $\text{Ba}_{0.6}\text{Sr}_{0.4}\text{TiO}_3$ were alternately ablated by the pulsed laser beam and deposited onto the substrates.

Before being introduced into the growth chamber, the substrates, polished on both sides, were ultrasonically cleaned sequentially with alcohol and acetone. The growth of the thin films was carried out under oxygen pressure of 10 Pa after the vacuum system reached $3 \times 10^{-3} \text{ Pa}$ by molecular pump while the substrates were heated to 750°C . The concentration of Au nanoparticles was adjusted by changing the angles of the fan-shaped chips of metal Au. In this study, one pure BST film and five Au:BST films with different Au concentrations were prepared. The thickness of the Au/BST thin films was measured to be about 120 nm by a surface profile measuring system (DEKTAK, USA).

The crystalline structure and crystallographic orientation of the Au:BST films were analysed by x-ray diffraction (XRD) with $\text{Cu K}\alpha$ radiation at 1.54 \AA , while the nature of the chemical bond of the films was analysed using x-ray photoelectron spectroscopy (XPS). The Au concentration of the films can be obtained approximately from the XPS data.

The third-order optical nonlinear properties were characterized by the single beam Z-scan technique, using a mode-locked Nd: yttrium-aluminium-garnet (YAG) laser with a wavelength of 532 nm and a pulse width of 10 ns as the light source. The laser beam was focused on the sample with a 120 mm focal length lens. The light intensity was 10 MW cm^{-2} at the focus. The Au:BST films would be damaged if the light intensity reaches 25 MW cm^{-2} . Energies of the transmitted and reference beams were simultaneously measured by an energy ratiometer (Rm6600, Laser Probe Corp) when the sample was scanned along the optic axis (the z -direction). The ratio of these energies was recorded to eliminate the effect of laser power fluctuation. The laser repetition rate was set to 1 Hz in order to reduce an accumulative thermal effect. The measurement system was calibrated using CS_2 as a standard.

3. Result and discussion

Figure 1 shows the XRD result of the Au:BST thin films on MgO (100) substrates. As can be seen, the Au/BST film consists of three different BST phases, which means the structure of BST in the films is polycrystalline. The average size of Au nanoparticles is about 16.9 nm calculated from the full width at half maximum (FWHM) of the Au(111) peak.

The Ba 3d, Ba 4d, Sr 3d, Ti 2p and Au 4f XPS spectra for one of the films are shown in figure 2. For all the measurements, the binding energies were corrected with reference to the assumed value of 284.6 eV for the resulting C 1s line from the absorbed hydrocarbon contamination. There are two peaks located at 793.8 and 778.9 eV in figure 2(a), which come from Ba $3d_{3/2}$ and Ba $3d_{5/2}$. Similarly, there are Ti $2p_{3/2}$ and $2p_{1/2}$ peaks shown in figure 2(c). The broad peak in figure 2(b) could be deconvoluted into two peaks at 132.6 eV and 134.3 eV, corresponding to Sr $3d_{5/2}$ and Sr $3d_{3/2}$. The Au $4f_{7/2}$ peak at 83.1 eV was also close to the Ba $4d_{5/2}$ and the $4d_{3/2}$ peaks shown in figure 2(d). The atomic ratio of Ba/Sr/Ti, which could be calculated from the XPS data, was approximately 0.56:0.42:1, approaching 0.6:0.4:1. And the Au concentration (represented by p), defined as $\text{Au}/(\text{Au}+\text{Ba}+\text{Sr}+\text{Ti})$, was calculated to be 11.9%. The binding energy and the chemical composition proved that the Au:BST films were formed successfully. The values of Au concentration for other samples were calculated to be 9.7%, 4.9%, 2.0% and 1.1% by the same method.

Figure 3 shows the linear absorption coefficient of the Au:BST nanocomposites with various Au concentrations as a function of the wavelength in the range from 400 to 800 nm. As shown, no absorption peak is observed for the pure BST film and the film with $p = 1.1\%$ shows a smooth and broad peak due to the SPR effect at around 570 nm. With an increase in Au concentration, the SPR absorption peak becomes obvious and shifts to slightly longer wavelengths (red-shift). When $p = 11.9\%$, the SPR absorption peak is located at around 595 nm. This behaviour is similar to a previous report on Au: Al_2O_3 [18]. When the Au concentration is low, the shape of the Au nanoparticles could be regarded as spherical. The absorption coefficient α can be expressed by the following equation [19, 20]:

$$\alpha = 9p \frac{\omega}{c} \varepsilon_d^{3/2} \frac{\varepsilon_m''}{(\varepsilon_m' + 2\varepsilon_d)^2 + \varepsilon_m''^2}, \quad (1)$$

where ε_m' and ε_m'' are the real and imaginary parts of the complex dielectric constant of the metal, and ε_d is the dielectric constant of the dielectric matrix. The absorption coefficient has a maximum where the condition $\varepsilon_d = -\varepsilon_m'/2$ is satisfied with the assumption that ε_m'' is neglected. The red-shift of the SPR may originate from the different particle sizes because the value of ε_m' will change with the size of Au nanoparticle. According to the Mie theory [21], the contraction of the crystal lattice of the particles would decrease with the size of the Au nanoparticle which causes a decrease in the resonance frequency of surface plasmon. Besides, the anisotropic effect of Au nanoparticles becomes obvious with the increase in Au concentration [11] and the shape of the Au nanoparticles could not be simplified

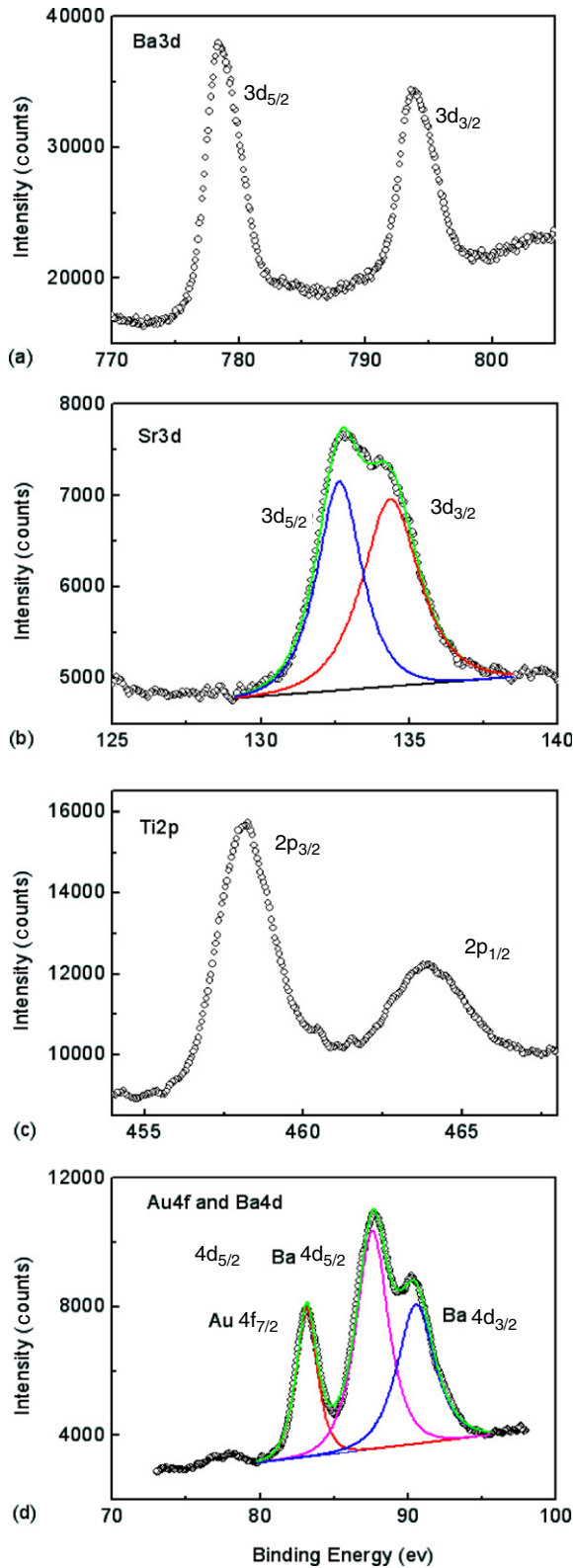


Figure 2. The x-ray photoelectron core-level spectra of (a) Ba 3d, (b) Sr 3d, (c) Ti 2p and (d) Au 4f, Ba 4d for the Au : BST film with Au concentration of 11.9%.

as spherical. So the resonant condition will change which may also contribute to red-shift phenomena.

The nonlinear absorption coefficient (β) and the nonlinear refractive index (n_2) [22] of the films were measured by the

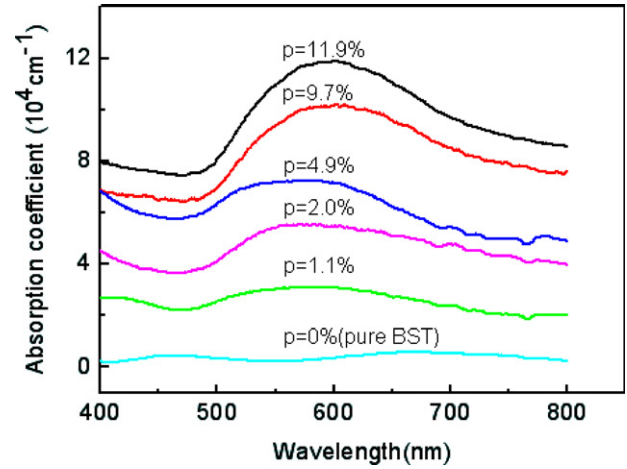


Figure 3. Curves of the absorption coefficient as a function of wavelength in the range from 400 to 900 nm depending on Au concentration.

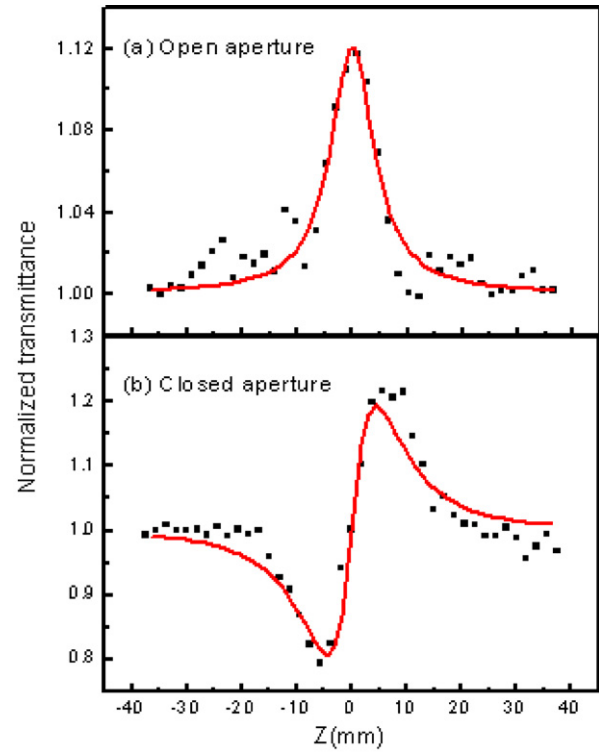


Figure 4. Z-scan measured curves of the film with the Au concentration of 11.9% for nonlinear optical absorption (a) and nonlinear refractive index (b). The solid lines are the theoretical fits.

Z-scan technique at 532 nm. A typical result of the Z-scan measurement for the Au ($p = 11.9\%$):BST nanocomposite film is shown in figure 4. The solid lines are a theoretical fit. It corresponds to the far field transmission of a Au : BST thin film as a function of its distance (z) to the lens focus.

The curve in figure 4(a), which comprises a normalized transmittance peak, indicates the presence of nonlinear saturation in the film because the shape of the Z-scan results for the MgO substrate is flat, which suggests that the nonlinear optical effect of substrates can be neglected. The nonlinear

absorption coefficient β (m/W), defined as $\alpha = \alpha_0 + \beta I$, where I is the intensity of light, can be calculated from the normalized transmittance for the open aperture by relation [16],

$$T(z, S=1) = \sum_{m=0}^{\infty} \frac{[-q_0(z)]^m}{(m+1)^{3/2}}, \quad (2)$$

where $q_0(z) = \beta I_0 L_{\text{eff}} / (1 + z^2/z_0^2)$, $L_{\text{eff}} = [1 - \exp(-\alpha L)]/\alpha$, the effective thickness of the film, $z_0 = k\omega_0^2/2$ the diffraction length, L the thickness of the film, α the linear absorption coefficient of the film and I_0 is the laser intensity at the focal point. Equation (2) can be simplified as

$$T(z, S=1) = 1 - \frac{\beta I_0 L_{\text{eff}}}{2\sqrt{2}(1 + z^2/z_0^2)}, \quad (3)$$

when $|q_0| < 1$, which was satisfied in our experiments.

The obtained β value for the Au : BST film was $-5.124 \times 10^{-5} \text{ m W}^{-1}$. The relation between the imaginary part of $\chi^{(3)}$ and β is as follows [23],

$$\text{Im}\chi^{(3)}(\text{esu}) = \frac{c^2 n_0^2}{120\pi^2 \omega} \beta (\text{m W}^{-1}), \quad (4)$$

where n_0 is the linear refractive index for Au : BST set as 2.3. Hence, the value of $\text{Im}\chi^{(3)}$ was calculated to be $-1.93 \times 10^{-6} \text{ esu}$.

The closed-aperture curve shown in figure 4(b) has a valley–peak configuration, which suggests that the value of the nonlinear refractive index is positive. It should be mentioned that the closed-aperture transmittance has been divided by the corresponding open-aperture data in order to neglect nonlinear absorption. The normalized transmittance in closed-aperture condition can be written as

$$T(z) \approx 1 + \frac{4\Delta\phi_0 x}{(x^2 + 1)(x^2 + 9)}, \quad (5)$$

where $x = z/z_0$. The nonlinear optical refractive index n_2 ($\text{m}^2 \text{ W}^{-1}$), defined as $n = n_0 + n_2 I$, was calculated using the following equation:

$$\Delta\phi_0 = kn_2 I_0 L_{\text{eff}}. \quad (6)$$

According to $I_0 = E_0/\pi\omega_0^2\tau$,

$$n_2 = \frac{\Delta\phi_0 z_0 \lambda^2 \tau}{2\pi E_0 L_{\text{eff}}}, \quad (7)$$

where $\Delta\phi_0$ was obtained from the theoretical fit.

The calculated n_2 of the Au : BST film was $1.309 \times 10^{-11} \text{ m}^2 \text{ W}^{-1}$. The real part of $\chi^{(3)}$ can be obtained by the following equation [23]:

$$\text{Re}\chi^{(3)}(\text{esu}) = cn_0^2 n_2 (\text{m}^2 \text{ W}^{-1}) / 120\pi^2, \quad (8)$$

where n_0 is the linear refractive index of Au : BST. The value of $\text{Re}\chi^{(3)}$ for the film ($p = 11.9\%$) was calculated to be $1.13 \times 10^{-5} \text{ esu}$, while the value of $\chi^{(3)}/\alpha$ is $1.13 \times 10^{-10} \text{ esu cm}$. Similarly, the values of $\text{Re}\chi^{(3)}$ for other samples ($p < 12\%$) were also determined as shown in figure 5. Since the laser

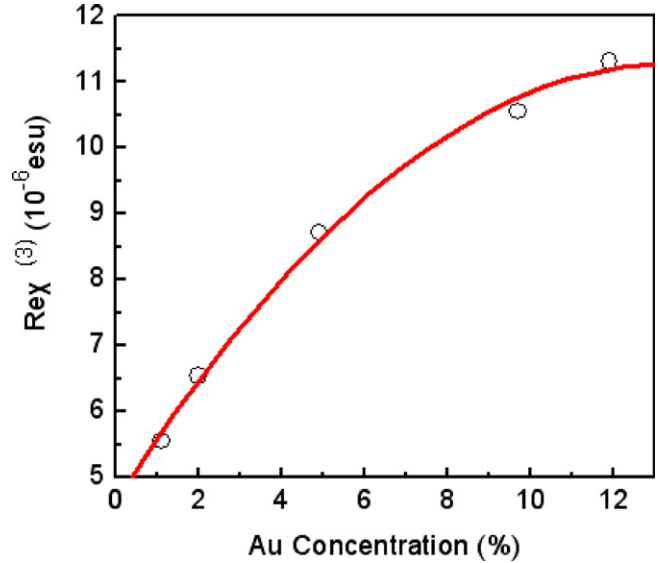


Figure 5. Curves of $\text{Re}\chi^{(3)}$ as a function of Au concentration.

would easily destroy the film if the Au concentration is too high, it is hard to obtain reliable values for the samples at a higher Au concentration. As can be seen, the value of $\text{Re}\chi^{(3)}$ is nearly proportional to the Au concentration when $p < 6\%$, and the curve becomes smoother at high Au concentrations, which means there may be a maximum value for $\text{Re}\chi^{(3)}$ and the value will probably decrease at higher Au concentrations. The relation between $\text{Re}\chi^{(3)}$ and metal concentration is similar to Au : Al_2O_3 [18]. These nonlinear optical properties at low Au concentrations can be interpreted by the following equation [24],

$$\chi^{(3)} = pf_1^2 |f_1|^2 \chi_m^{(3)} \quad (\text{when } p \text{ is small}), \quad (9)$$

where $\chi^{(3)}$ and $\chi_m^{(3)}$ are the third-order nonlinearity susceptibilities of the film and the Au nanoparticles, respectively, p the metal concentration and $f_1 = 3\varepsilon_d/(\varepsilon_m(\omega) + 2\varepsilon_h)$ the ratio between the internal field E_1 and the external field E_0 . It can be seen from equation (9) that $\chi^{(3)}$ is proportional to p when p is small, which is consistent with our result. As the Au concentration becomes larger, interaction among Au nanoparticles should be taken into account and then equation (9) would not hold true. In fact, Mackay has given a better interpretation by simulation for such homogenized composite mediums when p is large [25]. The simulation shows that the value of nonlinear permittivity would become larger with the increase in metal concentration under certain parameters. But it will become saturated and even decrease if metal concentration is too high, which is consistent with our experimental result.

It should be mentioned that the values of $\chi^{(3)}$ measured by the laser with a pulse width of several nanoseconds are usually about ten times as large as the ones measured by the laser with a pulse width of several picoseconds. The third-order nonlinear optical susceptibility of the Au : BST films is larger than those of Cu : BST [7] and BST [26]. It also compares favourably with the nonlinearities of some representative nonlinear optical materials, such as some transition-metal oxide thin films

(3.10×10^{-8} esu) [27], high density Cu-doped Al_2O_3 thin films (2.06×10^{-8} esu) [28] and organic polymer (1.07×10^{-7} esu) [29]. Hence, Au:BST film may be a promising candidate material for applications in nonlinear optical devices.

4. Conclusions

In summary, Au:BST thin films were grown on MgO (100) substrates by PLD. The XRD result shows that the structure of BST for the films is polycrystalline. There is characteristic SPR absorption at around 570 nm and the red-shift phenomenon is manifested when the Au concentration increases. The nonlinear optical properties of the films were investigated using the Z-scan method at the SPR wavelength. The values of the third-order susceptibility varied with the Au concentration and the relationship between the two was also analysed.

Acknowledgment

This work was supported by the National Key Basic Research Program of China, No 2006CB302905.

References

- [1] Vijayalakshmi S, Grebel H, Iqbal Z and White C W 1998 *J. Appl. Phys.* **84** 6502
- [2] Sakai J I 1992 *Phase Conjugate Optics* (Singapore: McGraw-Hill)
- [3] Shi W S, Chen Z H, Liu N N, Lu H B, Zhou Y L, Cui D F and Yang G Z 1999 *Appl. Phys. Lett.* **75** 1547
- [4] Wang W T, Yang G, Wu W D and Chen Z H 2003 *J. Appl. Phys.* **94** 6837
- [5] Yang G, Wang W T, Yan L, Lu H B, Yang G Z and Chen Z H 2002 *Opt. Commun.* **209** 445
- [6] Kim J-S, Lee K-S and Kim S S 2006 *Thin Solid Films* **515** 2332
- [7] Dalacu D and Martinu L 2000 *J. Appl. Phys.* **87** 228
- [8] Gehr R J and Boyd R W 1996 *Chem. Mater.* **8** 1807
- [9] Raether H 1971 *Surface Plasmons Oscillations and Their Applications in Physics of Thin Films* (New York: Academic)
- [10] Chakraborty P 1998 *J. Mater. Sci.* **33** 2235
- [11] Lakhtakia M N and Akhlesh Lakhtakia 2001 *Electromagnetics* **21** 129
- [12] Meldrum A, Haglund R F, Boatner L A and White C W 2001 *Adv. Mater.* **13** 1431
- [13] De G, Gusso M, Töpfer L, Catalano M, Gonella F, Mattei G, Mazzoldi P and Battaglin G 1996 *J. Appl. Phys.* **80** 6734
- [14] Liao H B, Xiao R F, Wang H, Wong K S and Wong G K L 1998 *Appl. Phys. Lett.* **72** 1817
- [15] Wang W T, Yang G, Chen Z H, Zhou Y L, Lu H B and Yang G Z 2002 *J. Appl. Phys.* **92** 7242
- [16] Sheik-Bahae M, Said A A, Wei T H, Hagan D J and Van Stryland E W 1990 *IEEE J. Quantum Electron.* **26** 760
- [17] Sheik-Bahae M, Said A A and Van Stryland E W 1989 *Opt. Lett.* **14** 955
- [18] Liao H B, Xiao R R, Fu J S and Wong G K L 1997 *Appl. Phys. B* **65** 673
- [19] Flytzanis C, Hache F, Kellin M C, Ricard D and Roussignol P H 1991 *Nonlinear Optics in Composite Materials Progress in Optics* (Amsterdam: North Holland)
- [20] Hache F, Ricard D and Flytzanis C 1986 *J. Opt. Soc. Am. B* **3** 1647
- [21] Russell B K, Mantovani J G, Anderson V E, Warmack R J and Ferrell T L 1987 *Phys. Rev. B* **35** 2151
- [22] Boyd R W 1992 *Nonlinear Optics* (San Diego, CA: Academic)
- [23] Chapple P B, Staromlynska J, Hermann J A and McKay T J 1991 *J. Nonlinear Opt. Phys. Mater.* **6** 251
- [24] Hache F, Ricard D, Flytzanis C and Kreibig U 1988 *Appl. Phys. A* **47** 347
- [25] Mackay T G 2005 *Electromagnetics* **25** 461
- [26] Wang W T, Dai Z H, Sun Y M, Sun Y P and Guan D Y 2005 *Appl. Surf. Sci.* **250** 268
- [27] Ando M, Kadono K, Haruta M, Sakaguchi T and Miya M 1995 *Nature* **374** 625
- [28] Ballesteros J M, Serna R, Solis J, Afonso C N, Petford-Long A K, Osborne D H and Haglund R F 1997 *Appl. Phys. Lett.* **71** 2445
- [29] Muto S, Kubo T, Kurokawa Y and Suzuki K 1998 *Thin Solid Films* **322** 233